



HAL
open science

Diaphragm shear modulus reflects transdiaphragmatic pressure Diaphragm shear modulus reflects transdiaphragmatic pressure 1 during isovolumetric inspiratory efforts and ventilation against inspiratory loading

Damien Bachasson, Martin Dres, Marie-Cecile Nierat, Jean-Luc Gennisson, Jean-Yves Hogrel, Jonne Doorduyn, Thomas Similowski

► To cite this version:

Damien Bachasson, Martin Dres, Marie-Cecile Nierat, Jean-Luc Gennisson, Jean-Yves Hogrel, et al.. Diaphragm shear modulus reflects transdiaphragmatic pressure Diaphragm shear modulus reflects transdiaphragmatic pressure 1 during isovolumetric inspiratory efforts and ventilation against inspiratory loading. *Journal of Applied Physiology*, 2019, 126 (3), pp.699-707. 10.1152/japphysiol.01060.2018 . hal-02272079

HAL Id: hal-02272079

<https://hal.sorbonne-universite.fr/hal-02272079>

Submitted on 27 Aug 2019

HAL is a multi-disciplinary open access archive for the deposit and dissemination of scientific research documents, whether they are published or not. The documents may come from teaching and research institutions in France or abroad, or from public or private research centers.

L'archive ouverte pluridisciplinaire **HAL**, est destinée au dépôt et à la diffusion de documents scientifiques de niveau recherche, publiés ou non, émanant des établissements d'enseignement et de recherche français ou étrangers, des laboratoires publics ou privés.

Diaphragm shear modulus reflects transdiaphragmatic pressure during isovolumetric inspiratory efforts and ventilation against inspiratory loading

Damien Bachasson^{*#1}, *Martin Dres*^{#2,3}, *Marie-Cécile Niérat*³, *Jean-Luc Gennisson*⁴, *Jean-Yves Hogrel*¹, *Jonne Doorduyn*⁵, *Thomas Similowski*^{2,3}

¹Institute of Myology, Neuromuscular Investigation Center, Neuromuscular Physiology Laboratory, Paris, France

²AP-HP, Groupe Hospitalier Pitié-Salpêtrière Charles Foix, Service de Pneumologie, Médecine Intensive et Réanimation, (*Département "R3S"*), F-75013, Paris, France

³Sorbonne Université, INSERM, UMRS1158 Neurophysiologie respiratoire expérimentale et clinique, F-75005 Paris, France

⁴Imagerie par Résonance Magnétique Médicale et Multi-Modalités (IR4M), CNRS UMR8081, Université Paris-Saclay, Orsay, France

⁵Department of Neurology, Donders Institute for Brain, Cognition and Behaviour, Radboud University Medical Center, Nijmegen, The Netherlands

[#]Both authors equally contributed to this work.

*Address for correspondence: Institute of Myology, Neuromuscular Investigation Center, Neuromuscular Physiology Laboratory, Hôpital Universitaire Pitié Salpêtrière, Paris 75651 Cedex 13, France. Tel: +33 1 42 16 66 41; fax: +33 1 42 16 58 81. E-mail address: d.bachasson@institut-myologie.org

Abstract

Aim. The reference method for the assessment of diaphragm function relies on the measurement of transdiaphragmatic pressure (Pdi). Local muscle stiffness measured using ultrafast shear wave elastography (SWE) provides reliable estimates of muscle force in locomotor muscles. This study aimed at investigating whether SWE could be used as a surrogate of Pdi to evaluate diaphragm function.

Methods. Fifteen healthy volunteers underwent a randomized step-wise inspiratory loading protocol of 0-60% of maximal isovolumetric inspiratory pressure during closed-airways maneuvers and 0-50% during ventilation against an external inspiratory threshold load. During all tasks, Pdi was measured and SWE was used to assess shear modulus of the right hemi-diaphragm (SMdi) at the zone of apposition. Pearson correlation coefficients (r) and repeated measures correlation coefficient (R) were computed to determine within individual and overall relationships between Pdi and SMdi, respectively.

Results. During closed-airways maneuvers, mean Pdi correlated to mean SMdi in all participants (r ranged from 0.77 to 0.96, all $p < 0.01$; $R = 0.82$, 95% CIs [0.76, 0.86], $p < 0.01$). During ventilation against inspiratory threshold loading, Pdi swing correlated to maximal SMdi in all participants (r ranged from 0.40 to 0.90, all $p < 0.01$; $R = 0.70$, 95% CIs [0.66, 0.73], $p < 0.001$). Changes in diaphragm stiffness as assessed by SWE reflect changes in transdiaphragmatic pressure.

Conclusion. SWE provides a new opportunity for direct and non-invasive assessment of diaphragm function.

37 **New & Noteworthy**

38 Accurate and specific estimation of diaphragm effort is critical for evaluating and monitoring diaphragm
39 dysfunction. The measurement of transdiaphragmatic pressure requires the use of invasive gastric and
40 esophageal probes. In the present work, we demonstrate that changes in diaphragm stiffness assessed with
41 ultrasound shear wave elastography reflect changes in transdiaphragmatic pressure, therefore offering a new
42 noninvasive method for gauging diaphragm effort.

43 **Introduction**

44 The evaluation and monitoring of respiratory muscle function in general and of diaphragm function in particular
45 are clinically relevant in a variety of clinical settings, among which weaning from mechanical ventilation (20).
46 Routine measurements of respiratory function like those of volumes, flows, and gas exchange, are nonspecific
47 and only give indirect information about respiratory muscle function. A more specific approach to
48 quantitatively assess respiratory muscle function relies on the measurement of their force producing capacity (1).
49 Yet there is currently no method directly giving access to respiratory muscle force in humans, hence the reliance
50 on pressure differences to assess respiratory muscle function. Likewise, the reference method for the assessment
51 of diaphragm function is the measurement of the transdiaphragmatic pressure (Pdi). Pdi is defined as the
52 difference between pleural and abdominal pressures that are inferred from esophageal pressure (Pes) and gastric
53 pressure (Pga), respectively (1). As the diaphragm is the only muscle that simultaneously lowers Pes and
54 increases Pga, Pdi is considered as the most specific approach to assess diaphragm function. Pdi is not a direct
55 reflection of diaphragm strength insofar as it depends on an array of factors governing the transformation of
56 force into pressure (such as lung volume as a determinant of diaphragm length, thoracic and abdominal
57 compliances, and thoracoabdominal configuration that can critically affect Pdi irrespective of any change in
58 diaphragm strength (5). Yet Pdi is clinically relevant in that it represents the actual force that drives lung volume
59 changes and therefore, ultimately, alveolar ventilation. Of note, measuring Pdi requires the use of esophageal
60 and gastric probes, which impedes its generalization as a clinical tool.

61 Diaphragm ultrasound imaging allows the noninvasive measurement of diaphragm excursion, thickness and
62 thickening (26, 31). Diaphragm thickening fraction has been shown to be an efficient tool for identifying
63 diaphragm dysfunction, monitoring its temporal changes, and predicting weaning outcomes in ventilated
64 patients (10, 11). However, equivocal relationships between Pdi and diaphragm thickening fraction have been
65 reported (12, 23, 29). Ultrasound shear wave elastography (SWE) is a recently available imaging method

66 allowing direct and real-time quantification of tissue mechanical properties (16). Briefly, SWE relies on the
67 measurement of propagation velocity of shear waves remotely generated inside tissues by ultrasonic focused
68 beams. Shear modulus can be readily estimated from the measured shear wave propagation velocity and tissue
69 density (4). Local muscle stiffness measured using SWE has been shown to provide reliable estimates of muscle
70 force in locomotor muscles (15, 18). Recently, Chino et al. (7) reported that the shear modulus of the diaphragm
71 (SMdi) increases along with mouth pressure (Pmo) during isovolumetric inspiratory efforts. However, the
72 relationship between SMdi and Pdi remains to be investigated.

73 Therefore, the aim of this study was to investigate the potential of ultrasound shear wave elastography to
74 evaluate diaphragm function in healthy subjects during isovolumetric inspiratory efforts and during ventilation
75 against inspiratory loads. We hypothesized that changes in SMdi would reflect changes in Pdi.

76 **Materials and Methods**

77 **Participants**

78 All participants gave written informed consent. This study conformed to the Declaration of Helsinki and was
79 approved by the local ethics committee (Comité de Protection des Personnes île-de-France VI, France). The
80 study was publicly registered prior to the first inclusion (ClinicalTrials.gov, NCT03313141).

81 **Experimental setup**

82 Participants were studied in a semirecumbent position (40 degrees) with uncast abdomen, breathing through a
83 mouthpiece while wearing a nose clip. The mouthpiece was connected to a two-way valve and
84 pneumotachograph (3700 series, linearity range 0–160 L*min⁻¹; Hans Rudolph, Kansas City, MO) for flow
85 measurement. Pmo was recorded using a differential transducer (model DP45–18, Validyne, Northridge, CA).
86 Pes and Pga were measured using 8-cm balloon catheters (C76080U; Marquat Génie Biomédical, Paris,

Diaphragm shear modulus reflects transdiaphragmatic pressure

France), connected separately to differential pressure transducers (model DP45-32; Validyne, Northridge, CA) as previously described (30). Flow and pressures signals were digitized (Powerlab, ADInstruments, Sydney, Australia) and recorded at a sampling frequency of 2 kHz (Labchart, ADInstruments). Pdi was obtained by online subtraction of Pes from Pga.

Ultrasound measurements. Diaphragm ultrasound imaging and shear wave elastography were performed using an Aixplorer Ultrasound scanner (V11.2, Supersonic Imagine, Aix-en-Provence, France) driving a 10-2 MHz linear transducer array (SL10-2, Supersonic Imagine). Settings were defined as follow: B-mode enabled; supersonic shear wave imaging mode enabled (SWE); penetration mode enabled; tissue tuner at $1540 \text{ m}\cdot\text{s}^{-1}$; dynamic range at 80 dB. Gain and time gain compensation were tailored for each patient. Sampling rates for B-mode imaging and SWE were 12 and 2 Hz, respectively. A generous amount of ultrasound gel was used during scanning for optimal acoustic coupling and minimal pressure was applied to the transducer in order to limit tissue deformation and modification of ventilatory mechanism. The right hemi-diaphragm was scanned at the zone of apposition, on the posterior axillary line vertical to the chest wall at the 8th-10th intercostal space. The right hemi-diaphragm was identified as a three-layered structure comprising two hyperechoic lines representing the pleural and peritoneal membranes and a middle hypoechoic layer representing the diaphragmatic muscle fibers. The rotation and angle of the transducer was then finely adjusted to obtain maximal echo intensity from diaphragmatic pleura and peritoneal membrane. The location of the probe was carefully marked on the skin to ensure reliable positioning of the probe within the protocol. Ultrasound acquisition were triggered with the Powerlab for synchronizing ultrasound, flow, and pressures recordings. Ultrasound measurements were performed by a trained operator (MD). An overview of the setup and samples of diaphragm ultrasound imaging is provided in Figure 1.

108 **Study protocol**

109 The study was carried out as follows: i) measurement of maximal isovolumetric inspiratory pressure (P_{Imax}), ii)
110 recordings during apnea at functional residual capacity (FRC), iii) recordings during inspiratory efforts against
111 closed airways, iv) recordings during ventilation against inspiratory threshold loading. Each step of the protocol
112 was performed twice.

113 *Maximal isovolumetric inspiratory pressure.* P_{Imax} was measured at FRC. At least five trials were performed
114 until three reproducible efforts, with less than 10% variance, were obtained (1). Maximal P_{mo} generated
115 amongst the three reproducible trials was defined as P_{Imax}.

116 *Apnea at FRC and isovolumetric inspiratory efforts against closed airways.* During these tasks, the mouthpiece
117 was disconnected from the three-way valve and flow was not monitored. Pressures and SM_{di} were measured
118 during ~5s open glottis apnea and during inspiratory efforts against closed airways at 10, 20, 30, 40, 50, and 60
119 % of P_{Imax}. Both apnea and inspiratory efforts were performed at FRC. Participants were asked to reach
120 progressively the target P_{mo} and to maintain their effort during ~10s. Visual feedback of generated P_{mo} and
121 guidelines were provided to participants using the built-in software option. Each task was repeated twice. Tasks
122 were alternated with 1-2 min of unloaded breathing.

123 *Ventilation against inspiratory threshold loading.* An in-house developed apparatus (23) modified from Chen et
124 al. (6) was used to perform ventilation against inspiratory threshold loads. Briefly, the device consisted of a
125 cylindrical adjustable pressure chamber connected to a non-rebreathing valve. The negative pressure was
126 generated by a commercially available vacuum cleaner. Pressure in the chamber (P_{ch}) was measured
127 continuously using a differential pressure transducer (model DP45-32; Validyne, Northridge, CA). The dead
128 space of the device was estimated at ~600 ml. Participants underwent a step-wise inspiratory threshold loading
129 protocol at 10, 20, 30, 40 and 50% of P_{Imax}. Each task was repeated twice. During each task, at least six
130 regular respiratory cycles were recorded. Tasks were alternated with 1-2 min of unloaded breathing.

131 **Data analysis**

132 Pes, Pga, Pdi, Pmo, Pch and flow were analyzed offline using standardized scripts in MATLAB (Mathworks,
 133 Natick, MA, USA). Frames from B-mode and SWE recordings were exported using the ultrasound scanner
 134 research pack (Soniclab, v12, Supersonic imagine) and each clips were processed offline using standardized
 135 scripts in MATLAB (Mathworks). A square region of interest (ROI) was drawn within the shear modulus map
 136 (see Figure 1) of the first frame of each clip between the diaphragmatic pleura and peritoneal. The latter ROI
 137 was replicated on other frames. SMdi was calculated assuming a linear elastic behavior in muscle tissue (4) as
 138 $SMdi = \rho \cdot V_s^2$ where ρ is the density of muscle ($1000 \text{ kg}\cdot\text{m}^{-3}$), and V_s is the shear wave speed in $\text{m}\cdot\text{s}^{-1}$. Values
 139 with each ROI were averaged and reported as SMdi. For measurements during isovolumetric inspiratory efforts,
 140 signals were manually selected when Pmo was stabilized at the targeted levels. Pressures and SMdi where then
 141 averaged over the duration of the selected period. During ventilation against inspiratory threshold loading,
 142 maximal SMdi and pressures variations (*i.e.* Pmo, Pes, Pga, Pdi) within inspiratory time were computed for
 143 each cycle. Cycles were discarded if diaphragm visualization was lost during the acquisition, or in the presence
 144 of lung artefacts. Mean SMdi at functional residual capacity during apnea was subtracted from mean SMdi or
 145 maximal SMdi (within inspiratory time) during isovolumetric efforts and ventilation, respectively.

146 **Statistics**

147 Data within text and tables are presented as mean \pm SD and mean [95% CIs] for correlation coefficients. The
 148 assumptions of normality and sphericity were confirmed using the D'Agostino's K-squared and Mauchly's
 149 tests, respectively. Repeated measures ANOVAs were conducted to evaluate change in variables depending on
 150 conditions. Tukey's HSD post-hoc tests were conducted when significant effect was found. Pearson correlation
 151 coefficients (r) were used for determining within-individual relationships between variables. For isovolumetric
 152 efforts, coefficients of variation were computed to assess the variability of Pdi and SMdi within the selected
 153 periods. Repeated measures correlation coefficient (R) were used for determining overall relationships between

variables (3). This statistical technique is used for determining the common within-individual association for paired measures assessed on two or more occasions for multiple individuals. This allows removing biases caused by violation of independence and/or differing patterns between-participants *versus* within-participants when performing simple correlation on aggregated data. All analyses were performed in the computing environment R version 3.2.4 (28). Statistical significance was set at $p < 0.05$ for all tests.

Results

Fifteen healthy participants (11 men, age = 32 years (min-max, 18-43), BMI = $24 \text{ kg}\cdot\text{m}^{-2}$ (SD 2.6); 4 women, age = 28 years (min-max, 20-44), BMI = $21.3 \text{ kg}\cdot\text{m}^{-2}$ (SD 1.3)) were studied. Mean P_{imax} was 120 cmH₂O (SD 26) and mean SM_{di} during apnea at FRC was 9.13 kPa (SD 2.17). Body weight and P_{imax} were significantly correlated ($r = 0.76$, $p < 0.01$).

Isovolumetric inspiratory effort against closed airways. Typical recordings from isovolumetric submaximal inspiratory efforts are shown in Figure 2 (see also Supplemental Video S1 [<https://figshare.com/s/eb987ad33ec4218e2cae>]). Two participants did not perform isovolumetric inspiratory efforts against closed airways and two participants did not performed 60% P_{imax}. Ultimately, the 89 available acquisitions were used for analysis. Mean selection duration for averaging data was 8.7 s (SD 3.9). Within selected data, mean of coefficient of variation for P_{mo}, P_{es}, P_{ga}, P_{di}, and SM_{di} were 14.2, 9.0, 6.3, 5.4, and 16.2 %, respectively. Pressures, and SM_{di} for all levels of inspiratory effort are displayed in Table 1 and Figure 3A. Repeated measures ANOVA showed significant effect of inspiratory effort levels on SM_{di} and P_{di}. Relationship between mean P_{di} swing and mean SM_{di} during all tasks for all data points is displayed in Figure 3B. Mean P_{di} significantly correlated to mean SM_{di} in all participants (r ranged from 0.77 to 0.96, all $p < 0.01$; $R = 0.82$, 95% CIs [0.76, 0.86]). Individual correlation coefficients and individual datapoints are shown in Table 2 and Figure 4, respectively.

176 *Ventilation against inspiratory threshold loading.* Typical recordings from ventilation against inspiratory
177 threshold loading in Figure 5 (see also Supplemental Video S2
178 [<https://figshare.com/s/28abd0263f7df2285b65>]). Two participants (5, 10) did not performed 50% P_{Imax}, one
179 participant did not performed 40% P_{Imax}, and one participant additionally performed 60% P_{Imax}). Ultimately,
180 66 cycles were discarded over 970-recorded cycles because of aberrant SM_{di} values caused by loss of
181 diaphragm visualization or lung artefacts during the acquisition. The number of cycles analyzed per loading
182 level was 11.8 (SD 3.0). Flow, Pressures, and SM_{di} for unloaded breathing and all levels of inspiratory levels
183 are displayed in Table 3 and Figure 6A. Repeated measures ANOVA showed significant effect of inspiratory
184 threshold loading levels on SM_{di} and P_{di}. Relationship between P_{di} swing and maximal SM_{di} for all analyzed
185 cycles and all loading tasks is displayed in Figure 6B. Maximal SM_{di} correlated to P_{di} swing in all participants
186 (r ranged from 0.40 to 0.90, all $p < 0.01$; $R = 0.70$, 95% CIs [0.66, 0.73], $p < 0.001$). Individual correlation
187 coefficients and individual datapoints are shown in Table 4 and Figure 7, respectively.

188 Discussion

189 The aim of the present study was to investigate the potential of ultrasound shear wave elastography for
190 evaluating diaphragm function in healthy subjects. We found that shear wave modulus of the diaphragm (*i.e.*
191 stiffness) was strongly correlated with transdiaphragmatic pressure during both isovolumetric inspiratory efforts
192 and inspiratory threshold loading.

193 As expected, increasing the inspiratory load during both isovolumetric inspiratory efforts and ventilation against
194 inspiratory threshold loading resulted in an increase in P_{di} (Table 1 and Figure 3; Table 3 and Figure 6,
195 respectively). It should be noted that during unloaded breathing, P_{di} and tidal volume were larger than expected
196 for healthy subjects (Table 3) (9). This is most likely the result of the additional resistance and instrumental
197 dead space imposed by the experimental device. Accordingly, variations in P_{mo} expressed as a percentage of

Diaphragm shear modulus reflects transdiaphragmatic pressure

198 P_{lmax} were greater than pressure within the inspiratory loading device. Our data showed strong linear
199 relationship between mean SM_{di} and P_{di} during submaximal isovolumetric inspiratory efforts (Figure 3). These
200 findings demonstrate that diaphragm stiffening is strongly related to the level of diaphragm activation as
201 assessed by P_{di} measurements. These findings are in line with the repeatedly demonstrated linear relationship
202 between muscle shear modulus and active muscle force in locomotor muscles (2, 15, 18, 21). These results are
203 also in agreement with the recent work by Chino et al. (7) that reported significant correlation between SM_{di}
204 and P_{mo} during similar isovolumetric inspiratory efforts at FRC. However, we reported lower SM_{di} values for
205 given isovolumetric inspiratory efforts *e.g.* mean SM_{di} was 63 kPa (SD 16) at 50% of P_{lmax} *versus* 29 kPa (SD
206 13) in the present work. Diaphragm recruitment is known to be reduced during voluntary inspiratory efforts in
207 the semirecumbent position compared to the sitting position that was used in the study by Chino et al. (19). A
208 lower ability of the participants to efficiently recruit their diaphragm may also contributed to explain these
209 results. Our data also show strong linear relationship between max SM_{di} and P_{di} swing during ventilation
210 against inspiratory threshold loading. These findings demonstrate for the first time that diaphragm function can
211 be noninvasively monitored using SWE during breathing. Besides one report in the cardiac muscle (8), this is
212 also the first report supporting that SWE may be used to monitor dynamic muscle contractions. Although we
213 found high individual correlation coefficients between SM_{di} and P_{di} in most participants, our data showed that
214 SM_{di} may fail to increase along with P_{di} during both isovolumetric inspiratory efforts (*i.e.* participants 5, 11,
215 12; Figure 4 and Table 2) and during ventilation against inspiratory threshold loading (*i.e.* participants 5, 12, 15;
216 Figure 7 and Table 4). These findings may be explained, at least in part, by misalignment of the transducer
217 according to the direction of diaphragm fascicles. This factor has been repeatedly identified as critical given the
218 highly anisotropic nature of the skeletal muscle (17). Slight offset of transducer angle in reference to the
219 direction of muscle fascicles reduces shear modulus value (17). Therefore, quality criteria for SM_{di}
220 measurements must be established and adjustment of transducers in the three-dimensional space shall be
221 assisted programmatically to obtain largest SM_{di} changes during ventilation. Another potential explanation is

Diaphragm shear modulus reflects transdiaphragmatic pressure

that Pdi is an indirect reflect of diaphragm force, insofar as the its generation is influenced by factors such as lung volume, thoracoabdominal compliances and thoracoabdominal geometrical configuration (see introduction). Also, Pdi can be contributed to by extra diaphragmatic inspiratory muscles or by expiratory muscles if the transmission of the pressure that these muscle generate across the diaphragm is incomplete, which can occur in the presence of concomitant contraction of the diaphragm with other respiratory muscles (14, 27). Thus, high Pdi values can be reached in certain circumstances with limited contribution of the diaphragm. Interestingly, we observed less steep relationship between SMdi and Pdi during isovolumetric effort as compared to ventilation against threshold inspiratory loading. This may be explained, at least in part, by the fact that efforts were performed at functional residual capacity during submaximal isovolumetric effort *i.e.* closer to diaphragm optimal length as compared to ventilation against threshold inspiratory loading where peak Pdi is reached at higher pulmonary volume.

Limitations. Participants were free to use any strategy to reach the target during isovolumetric inspiratory effort (with a Pmo rather that a Pdi target) or to overcome inspiratory loads during ventilation tasks. This may have led to poor diaphragm recruitment. Within the present study, SWE frame rate was limited to 2 Hz and this may contribute, at least in part, to reduce the amplitude of SMdi variations. Increase in SWE frame rate represents a critical challenge to fully exploit the potential of SMdi measurements. Oppersma et al. (23) recently demonstrated that diaphragm strain and strain rate assessed using speckle tracking outperform conventional ultrasound methods. Comparison of SMdi with strain-derived metrics and conventional thickening fraction remain to be investigated. Ultrasound muscle imaging is highly operator dependent. Change in transducer position might have occurred, in particularly with large thorax movement and this may contribute to explain inferior SWE performance in some participants. As previously observed during pretests, SMdi could not be assessed during maximal inspiratory maneuvers. It is unlikely that diaphragm SWE may be accurately used as performed within this study during maximal inspiratory maneuvers because of sudden thorax movement and large diaphragm deformation. Collectively, these findings emphasize the need to develop specifically designed

Diaphragm shear modulus reflects transdiaphragmatic pressure

246 skin-transducer interfaces and optimized post processing methods for reducing these confounding effects. In
247 addition, both intra- and inter-operator reliability of SMdi measurements remain to be evaluated. The limited
248 frame rate of SWE mentioned above also prevent the use of SWE during electrical/magnetic phrenic nerve
249 stimulation or brief volitional maneuvers such as the sniff test (1). Although SWE frame rate may be
250 substantially increased (8), it will most likely remain too low for capturing such short events because shear
251 waves must first travel through the tissue to be filmed (16). Similarly to conventional ultrasound methods, lung
252 sliding may block a good view on the diaphragm when tidal volume increases (26). This may therefore prevent
253 us from using diaphragm SWE when ventilatory demand is increased *e.g.* during exercise and/or with higher
254 inspiratory volume. This will be investigated in future works. At last, increase diaphragm depth caused by
255 thicker subcutaneous tissue in overweighed patients may also affect SMdi measurements (13).

256 *Perspective and clinical implications.* Diaphragm SWE appears to have a strong potential for direct,
257 noninvasive, and specific assessment of diaphragm effort. SMdi coupled with functional respiratory
258 investigations may help to detect diaphragm dysfunction (25). Although feasibility of diaphragm SWE in the
259 left zone of apposition (and other approaches) remain to be investigated, it might be particularly useful for
260 detecting diaphragm hemi-paralysis. Diaphragm SWE might also be particularly relevant within spontaneous
261 breathing trials and/or pressure support ventilation in ventilated patients during the weaning phase (22, 25).
262 Diaphragm stiffening-time index may also be computed during spontaneous breathing trial similarly to the
263 diaphragm excursion-time index recently proposed by Palkar et al. (24). Hence the feasibility and the
264 performance of SMdi measurements in critically ill patients shall be assessed in future studies. Pediatric use of
265 diaphragm SWE also remain to be addressed. The current offline setting of the data analysis impedes the use of
266 diaphragm SWE at the bedside. Built-in mode must be developed within ultrasound scanners to allow on-site
267 SMdi measurements. The development of a device specifically designed for this purpose may also help to apply
268 and disseminate the use of diaphragm SWE.

269 In conclusion, diaphragm SWE may be used as a noninvasive and specific method for detecting stepwise
270 increases in diaphragm effort during submaximal isovolumetric inspiratory efforts and during ventilation
271 against inspiratory threshold loading. SMdi was strongly correlated to Pdi within both models. Further research
272 and technological developments are required to optimize diaphragm SWE and its conditions of use for the
273 diagnosis and follow up of diaphragm dysfunction as well as its potential for predicting weaning outcome in the
274 ventilated patient.

275 **Acknowledgments**

276 We gratefully thank all the volunteers who participated in this study. This study was supported by the
277 Association pour le Développement et l'Organisation de la Recherche en Pneumologie et sur le Sommeil
278 (ADOREPS), the program Investissement d'Avenir ANR-10-AIHU 06 of the French Government, and the
279 Association Française Contre Les Myopathies (AFM).

280 **Conflict of Interest**

281 JLG is a scientific consultant for Supersonic Imagine, Aix-en-Provence, France. MD received personal fees
282 from Lungpacer Medical Inc., Vancouver, Canada. A request for a patent that encompasses findings presented
283 in the present work has been filled.

References

1. **American Thoracic Society/European Respiratory S.** ATS/ERS Statement on respiratory muscle testing. *American Journal of Respiratory and Critical Care Medicine* 166: 518-624, 2002.
2. **Ates F, Hug F, Bouillard K, Jubeau M, Frappart T, Couade M, Bercoff J, and Nordez A.** Muscle shear elastic modulus is linearly related to muscle torque over the entire range of isometric contraction intensity. *Journal of Electromyography and Kinesiology* 25: 703-708, 2015.
3. **Bakdash JZ, and Marusich LR.** Repeated Measures Correlation. *Front Psychol* 8: 456, 2017.
4. **Bercoff J, Tanter M, and Fink M.** Supersonic shear imaging: a new technique for soft tissue elasticity mapping. *IEEE Transactions on Ultrasonics Ferroelectrics and Frequency Control* 51: 396-409, 2004.
5. **Chen R, Kayser B, Yan S, and Macklem PT.** Twitch transdiaphragmatic pressure depends critically on thoracoabdominal configuration. *J Appl Physiol (1985)* 88: 54-60, 2000.
6. **Chen RC, Que CL, and Yan S.** Introduction to a new inspiratory threshold loading device. *Eur Respir J* 12: 208-211, 1998.
7. **Chino K, Ohya T, Katayama K, and Suzuki Y.** Diaphragmatic shear modulus at various submaximal inspiratory mouth pressure levels. *Respir Physiol Neurobiol* 252-253: 52-57, 2018.
8. **Couade M, Pernot M, Messas E, Bel A, Ba M, Hagege A, Fink M, and Tanter M.** In vivo quantitative mapping of myocardial stiffening and transmural anisotropy during the cardiac cycle. *IEEE Transactions on Medical Imaging* 30: 295-305, 2011.
9. **Doorduyn J, Sinderby CA, Beck J, Stegeman DF, van Hees HW, van der Hoeven JG, and Heunks LM.** The calcium sensitizer levosimendan improves human diaphragm function. *American Journal of Respiratory and Critical Care Medicine* 185: 90-95, 2012.

- 305 10. **Dres M, Goligher EC, Dube BP, Morawiec E, Dangers L, Reuter D, Mayaux J, Similowski T, and**
306 **Demoule A.** Diaphragm function and weaning from mechanical ventilation: an ultrasound and phrenic nerve
307 stimulation clinical study. *Ann Intensive Care* 8: 53, 2018.
- 308 11. **Dube BP, and Dres M.** Diaphragm Dysfunction: Diagnostic Approaches and Management Strategies.
309 *Journal of Clinical Medicine* 5: 113, 2016.
- 310 12. **Dube BP, Dres M, Mayaux J, Demiri S, Similowski T, and Demoule A.** Ultrasound evaluation of
311 diaphragm function in mechanically ventilated patients: comparison to phrenic stimulation and prognostic
312 implications. *Thorax* 72: 811-818, 2017.
- 313 13. **Ewertsen C, Carlsen JF, Christiansen IR, Jensen JA, and Nielsen MB.** Evaluation of healthy muscle
314 tissue by strain and shear wave elastography - Dependency on depth and ROI position in relation to underlying
315 bone. *Ultrasonics* 71: 127-133, 2016.
- 316 14. **Gandevia SC, McKenzie DK, and Plassman BL.** Activation of human respiratory muscles during
317 different voluntary manoeuvres. *J Physiol* 428: 387-403, 1990.
- 318 15. **Gennisson JL, Cornu C, Catheline S, Fink M, and Portero P.** Human muscle hardness assessment
319 during incremental isometric contraction using transient elastography. *Journal of Biomechanics* 38: 1543-1550,
320 2005.
- 321 16. **Gennisson JL, Deffieux T, Fink M, and Tanter M.** Ultrasound elastography: principles and
322 techniques. *Diagn Interv Imaging* 94: 487-495, 2013.
- 323 17. **Gennisson JL, Deffieux T, Mace E, Montaldo G, Fink M, and Tanter M.** Viscoelastic and
324 anisotropic mechanical properties of in vivo muscle tissue assessed by supersonic shear imaging. *Ultrasound in*
325 *Medicine and Biology* 36: 789-801, 2010.
- 326 18. **Hug F, Tucker K, Gennisson JL, Tanter M, and Nordez A.** Elastography for Muscle Biomechanics:
327 Toward the Estimation of Individual Muscle Force. *Exercise and Sport Sciences Reviews* 43: 125-133, 2015.

- 328 19. **Koulouris N, Mulvey DA, Laroche CM, Goldstone J, Moxham J, and Green M.** The effect of
329 posture and abdominal binding on respiratory pressures. *Eur Respir J* 2: 961-965, 1989.
- 330 20. **Laghi F, and Tobin MJ.** Disorders of the respiratory muscles. *American Journal of Respiratory and*
331 *Critical Care Medicine* 168: 10-48, 2003.
- 332 21. **Lapole T, Tindel J, Galy R, and Nordez A.** Contracting biceps brachii elastic properties can be
333 reliably characterized using supersonic shear imaging. *European Journal of Applied Physiology* 115: 497-505,
334 2015.
- 335 22. **Magalhaes PAF, Camillo CA, Langer D, Andrade LB, Duarte M, and Gosselink R.** Weaning failure
336 and respiratory muscle function: What has been done and what can be improved? *Respiratory Medicine* 134:
337 54-61, 2018.
- 338 23. **Oppersma E, Hatam N, Doorduyn J, van der Hoeven JG, Marx G, Goetzenich A, Fritsch S,**
339 **Heunks LMA, and Bruells CS.** Functional assessment of the diaphragm by speckle tracking ultrasound during
340 inspiratory loading. *J Appl Physiol (1985)* 123: 1063-1070, 2017.
- 341 24. **Palkar A, Narasimhan M, Greenberg H, Singh K, Koenig S, Mayo P, and Gottesman E.**
342 Diaphragm Excursion-Time Index: A New Parameter Using Ultrasonography to Predict Extubation Outcome.
343 *Chest* 153: 1213-1220, 2018.
- 344 25. **Pirompanich P, and Romsaiyut S.** Use of diaphragm thickening fraction combined with rapid shallow
345 breathing index for predicting success of weaning from mechanical ventilator in medical patients. *J Intensive*
346 *Care* 6: 6, 2018.
- 347 26. **Sarwal A, Walker FO, and Cartwright MS.** Neuromuscular ultrasound for evaluation of the
348 diaphragm. *Muscle & Nerve* 47: 319-329, 2013.
- 349 27. **Similowski T, Duguet A, Straus C, Attali V, Boisteanu D, and Derenne JP.** Assessment of the
350 voluntary activation of the diaphragm using cervical and cortical magnetic stimulation. *Eur Respir J* 9: 1224-
351 1231, 1996.

- 352 28. **Team RC.** R: A Language and Environment for Statistical Computing. 2017.
- 353 29. **Umbrello M, Formenti P, Longhi D, Galimberti A, Piva I, Pezzi A, Mistraletti G, Marini JJ, and**
354 **Iapichino G.** Diaphragm ultrasound as indicator of respiratory effort in critically ill patients undergoing
355 assisted mechanical ventilation: a pilot clinical study. *Critical Care* 19: 161, 2015.
- 356 30. **Verges S, Bachasson D, and Wuyam B.** Effect of acute hypoxia on respiratory muscle fatigue in
357 healthy humans. *Respiratory Research* 11: 109, 2010.
- 358 31. **Zambon M, Greco M, Bocchino S, Cabrini L, Beccaria PF, and Zangrillo A.** Assessment of
359 diaphragmatic dysfunction in the critically ill patient with ultrasound: a systematic review. *Intensive Care*
360 *Medicine* 43: 29-38, 2017.

361

Tables

Table 1. Pressures and diaphragm shear modulus during apnea and during isovolumetric inspiratory efforts against closed airways.

variables	target (%P _I max)						
	0	10	20	30	40	50	60
mean P _{mo} (% P _I max)	-	10.2 (1.6)	19.0 (1.9)*	29.1 (2.5)*	39.1 (3.2)*	47.7 (3.0)*	56.5 (4.8)*
mean P _{es} (cmH ₂ O)	3.8 (2.9)	-8.8 (5.3)	-16.7 (9.0)*	-26.8 (12.4)*	-37.1 (16.3)*	-45.6 (20.7)*	-55.8 (19.4)*
mean P _{ga} (cmH ₂ O)	10.9 (2.9)	16.9 (9.5)*	14.7 (3.8)*	16.2 (5.4)*	15.6 (5.1)*	17.6 (6.6)*	17.0 (9.8)*
mean P _{di} (cmH ₂ O)	14.8 (3.5)	25.8 (11.1)*	31.4 (10.3)*	43.0 (12.6)*	52.7 (16.7)*	63.1 (20.7)*	72.9 (24.8)*
mean SM _{di} (kPa)	0.6 (0.6)	7.3 (6.0)*	9.0 (6.5)*	15.2 (9.7)*	18.7 (9.9)*	25.9 (9.7)*	28.9 (12.6)*

Data are shown as mean (SD). Data from two trials for each condition were averaged. Target (% P_Imax), targeted pressure expressed as a percentage of maximal voluntary isovolumetric inspiratory pressure with 0% P_Imax corresponding to measurements during apnea at functional residual capacity ; mean P_{mo} (% P_Imax), mean mouth pressure expressed as a percentage of P_Imax; P_{es}, esophageal pressure; P_{ga}, gastric pressure; P_{di}, transdiaphragmatic pressure, SM_{di}, diaphragm shear modulus.*significantly different from 0% P_Imax ($p < 0.05$).

371 **Table 2.** Relationship between diaphragm shear modulus during isovolumetric inspiratory efforts against closed
 372 airways in all participants.

Participants	<i>r</i> [95% CI]	<i>p</i> value
1	0.79 [0.39-0.94]	< 0.01
2	0.87 [0.64-0.96]	< 0.001
3	0.92 [0.77-0.98]	< 0.001
4	0.91 [0.73-0.97]	< 0.001
5	0.92 [0.76-0.97]	< 0.001
6	0.92 [0.76-0.97]	< 0.001
7	0.86 [0.60-0.95]	< 0.001
8	0.95 [0.84-0.98]	< 0.001
9	0.88 [0.67-0.96]	< 0.001
10	0.77 [0.31-0.94]	< 0.01
11	0.96 [0.88-0.99]	< 0.001
12	0.80 [0.47-0.93]	< 0.001
13	0.85 [0.58-0.95]	< 0.001

373 *r* [95% CI], Pearson correlation coefficient with lower and higher 95% confidence intervals.

Diaphragm shear modulus reflects transdiaphragmatic pressure

374 **Table 3.** Flow, pressures, and diaphragm shear modulus during unloaded ventilation and ventilation against
 375 inspiratory threshold loading.

variables	threshold loading (% P _I max)					
	0	10	20	30	40	50
Bf (breaths/min)	12.0 (2.2)	13.3 (2.8)	12.3 (2.8)	12.9 (3.1)	12.3 (3.0)	12.9 (4.2)
EE Pes (cmH₂O)	4.3 (2.8)	2.8 (2.0)	2.4 (2.6)	4.1 (1.8)	6.3 (4.0)	7.1 (3.7)*
V_T (l)	0.5 (0.7)	0.8 (0.7)	0.8 (0.8)	0.6 (0.7)	0.6 (0.8)	0.5 (0.7)
T_I (s)	2.1 (0.3)	2.5 (0.5)	2.8 (0.6)	2.8 (0.6)	2.9 (0.8)	3.0 (1.0)
V_T/T_I	0.2 (0.3)	0.4 (0.4)	0.3 (0.3)	0.2 (0.3)	0.2 (0.3)	0.2 (0.3)
T_I/T_T	0.4 (0.0)	0.5 (0.1)	0.6 (0.1)	0.6 (0.1)	0.6 (0.1)	0.6 (0.1)
mean Pch (cmH₂O)	4.1 (1.3)	-12.9 (2.7)*	-24.4 (5.8)*	-36.4 (9.2)*	-48.2 (10.8)*	-59.2 (14.4)*
Δ P_{mo} (% P_Imax)	1.7 (0.5)	19.6 (2.6)*	29.6 (3.6)*	39.0 (4.5)*	46.6 (6.6)*	54.2 (9.3)*
Δ Pes (cmH₂O)	-8.5 (2.6)	-27.2 (9.9)	-38.4 (14.6)*	-48.2 (16.1)*	-60.4 (18.9)*	-67.8 (21.5)*
Δ P_{ga} (cmH₂O)	6.3 (2.2)	7.6 (5.2)	9.9 (6.1)*	10.1 (4.7)*	8.8 (2.6)*	8.7 (2.2)*
Δ P_{di} (cmH₂O)	10.4 (4.4)	29.8 (13.8)*	42.3 (18.3)*	49.4 (17.9)*	59.1 (20.9)*	63.6 (23.1)*
max SM_{di} (kPa)	6.2 (3.6)	16.0 (8.5)*	24.3 (10.0)*	27.8 (13.8)*	32.5 (13.8)*	35.7 (13.4)*

376 Data are shown as mean (SD). Data from each cycle for a given loading level were averaged. Threshold loading
 377 (% P_Imax), inspiratory threshold loading expressed as a percentage of maximal voluntary isovolumetric
 378 inspiratory pressure with 0% P_Imax corresponding to unloaded ventilation; Bf, breathing frequency; EE Pes,
 379 end-expiratory esophageal pressure; V_T, tidal volume; T_I, inspiratory time; V_T /T_I, tidal volume to inspiratory
 380 time ratio *i.e.* inspiratory flow; T_I/T_T, ratio of inspiratory to total time of the respiratory cycle *i.e.* duty cycle;
 381 mean Pch, mean chamber pressure within the inspiratory loading device. P_{mo}, variation of mouth pressure
 382 during inspiratory time; Δ P_{mo}, variation of mouth pressure during inspiratory time; Δ Pes, variation of
 383 esophageal pressure during inspiratory time; Δ P_{ga}, variation of gastric pressure during inspiratory time; Δ P_{di},
 384 variation of transdiaphragmatic pressure during inspiratory time; max SM_{di}, maximal diaphragm shear modulus

Diaphragm shear modulus reflects transdiaphragmatic pressure

385 during the inspiratory time. TFdi, diaphragm thickening fraction. *significantly different from unloaded
386 breathing *i.e.* threshold loading 0 % PImax ($p < 0.05$).

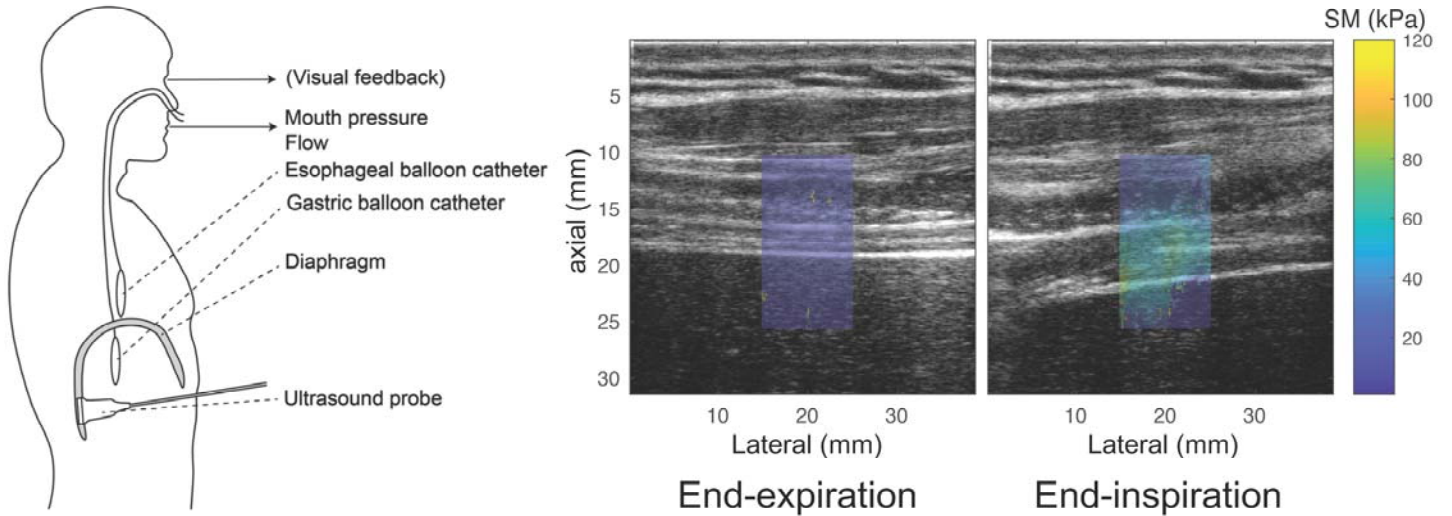
387 **Table 4.** Relationship between diaphragm shear modulus during unloaded ventilation and ventilation against
 388 inspiratory threshold loading in all participants.

Participants	<i>r</i> [95% CI]	<i>p</i> value
1	0.73 [0.59-0.83]	< 0.001
2	0.85 [0.76-0.90]	< 0.001
3	0.90 [0.84-0.94]	< 0.001
4	0.90 [0.84-0.94]	< 0.001
5	0.40 [0.18-0.59]	< 0.001
6	0.79 [0.68-0.86]	< 0.001
7	0.86 [0.77-0.91]	< 0.001
8	0.87 [0.80-0.92]	< 0.001
10	0.55 [0.21-0.78]	< 0.01
12	0.44 [0.22-0.61]	< 0.001
13	0.67 [0.47-0.80]	< 0.001
14	0.82 [0.73-0.89]	< 0.001
15	0.76 [0.64-0.85]	< 0.001

389 *r* [95% CI], Pearson correlation coefficient with lower and higher 95% confidence intervals.

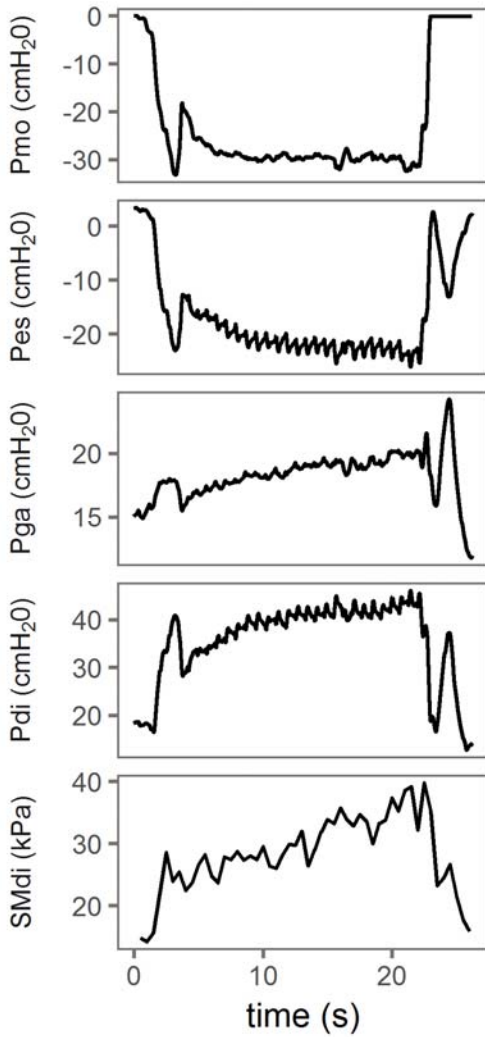
Figures

Figure 1. Overview of the experimental setup.



The left panel shows the experimental setup with respiratory measurements and intercostal diaphragm ultrasound imaging. Visual feedback of generated mouth pressure and guidelines were provided during isovolumetric inspiratory efforts against closed airways. The right panel shows the shear modulus (SM) map in kPa measured using shear wave elastography overlaid with standard B-Mode at end-expiration and end-inspiration during ventilation against inspiratory threshold loading.

398 **Figure 2.** Typical measurements during isovolumetric inspiratory efforts against closed airways in participant
399 #3.

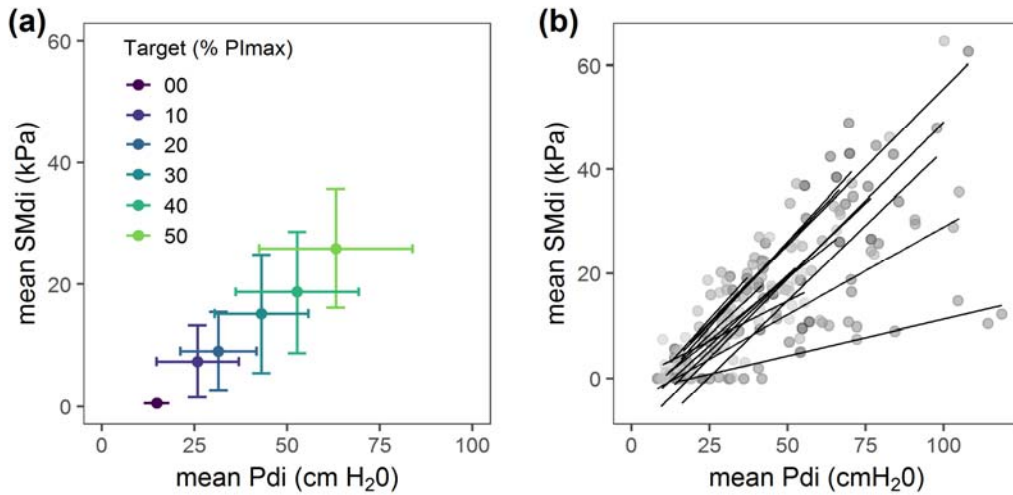


400

401 Pmo, mouth pressure; Pes, esophageal pressure; Pga, gastric pressure; Pdi, transdiaphragmatic pressure, SMdi,
402 diaphragm shear modulus.

403

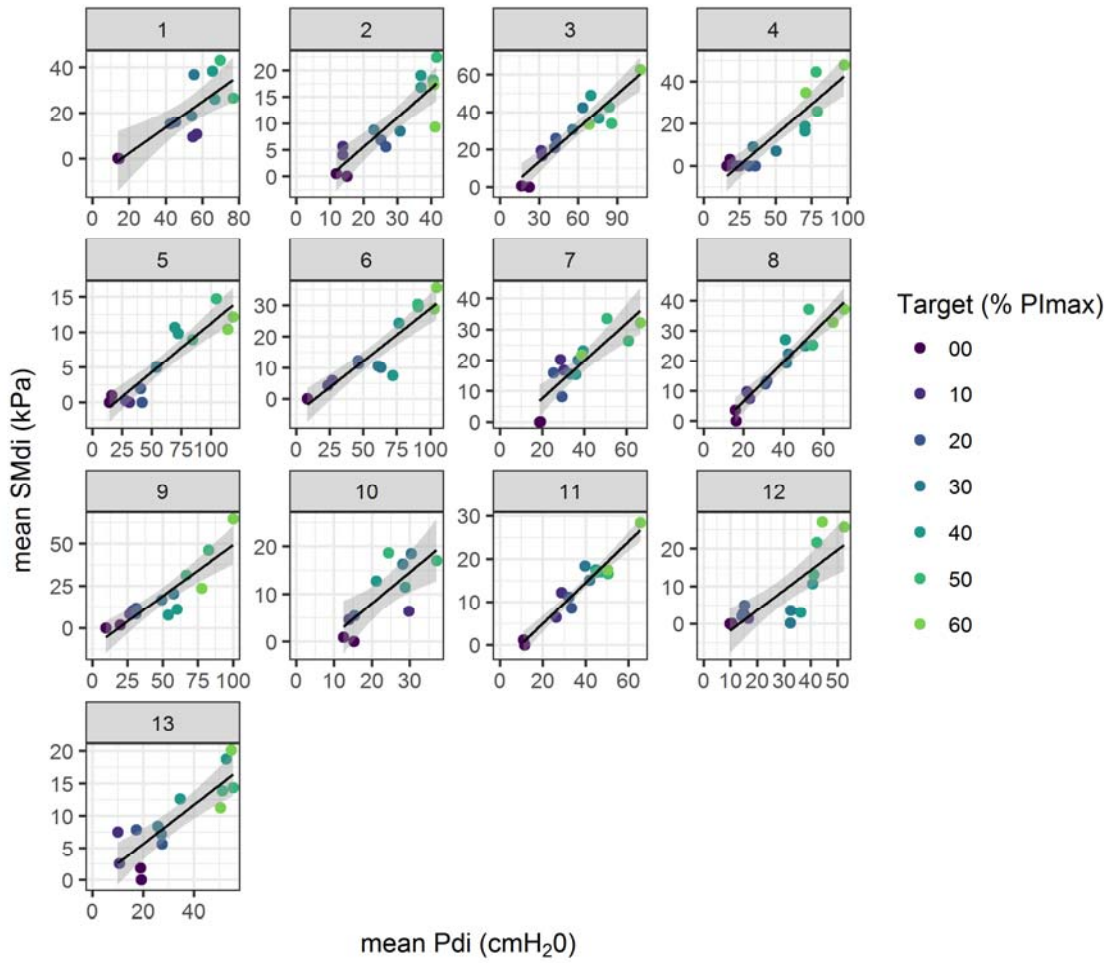
404 **Figure 3.** Relationship between transdiaphragmatic pressure and diaphragm shear modulus during submaximal
405 isovolumetric inspiratory efforts against closed airways (n=13).



406
407 Panel (a): average values per condition i.e. apnea at functional residual capacity and submaximal isovolumetric
408 inspiratory efforts at 10, 20, 30, 40, 50 % of maximal inspiratory pressure (PI max). Panel (b): all data points
409 with individual linear regression lines; mean SMdi, mean diaphragm shear modulus; mean Pdi, mean
410 transdiaphragmatic pressure.

Diaphragm shear modulus reflects transdiaphragmatic pressure

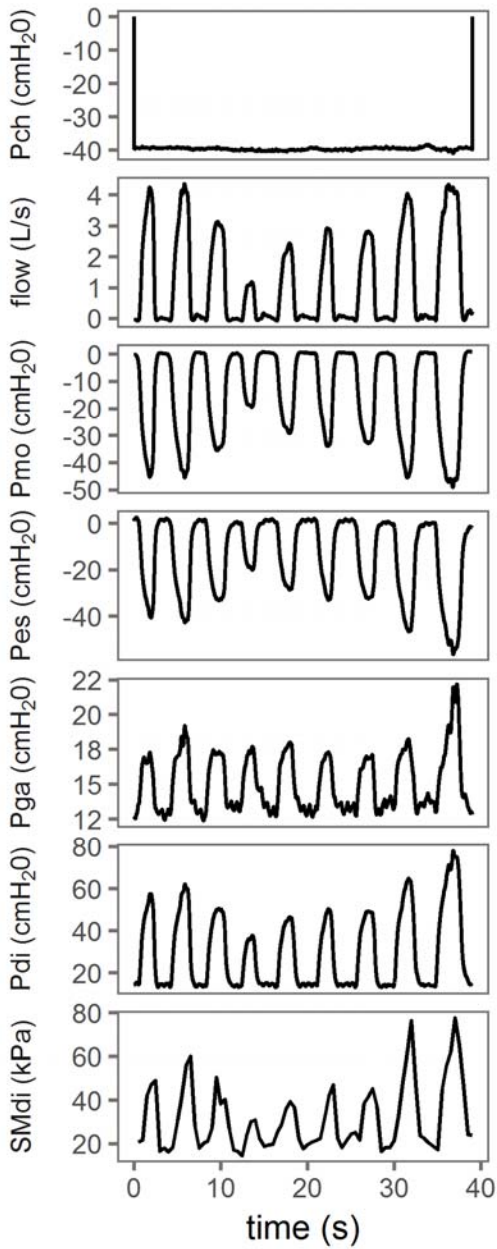
411 **Figure 4.** Individual data points illustrating relationship between transdiaphragmatic pressure and diaphragm
412 shear modulus during submaximal isovolumetric inspiratory efforts against closed airways.



413

414

415 **Figure 5.** Typical measurements during ventilation against inspiratory threshold loading in participant #1.

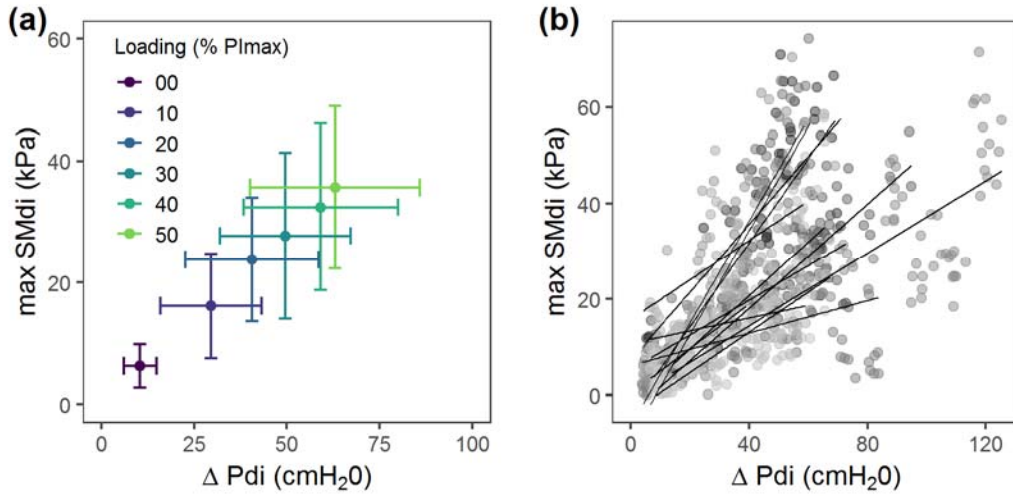


416

417 Pch, chamber pressure with the inspiratory threshold loading device; Pmo, mouth pressure; Pes, esophageal

418 pressure; Pga, gastric pressure; Pdi, transdiaphragmatic pressure, SMdi, diaphragm shear modulus.

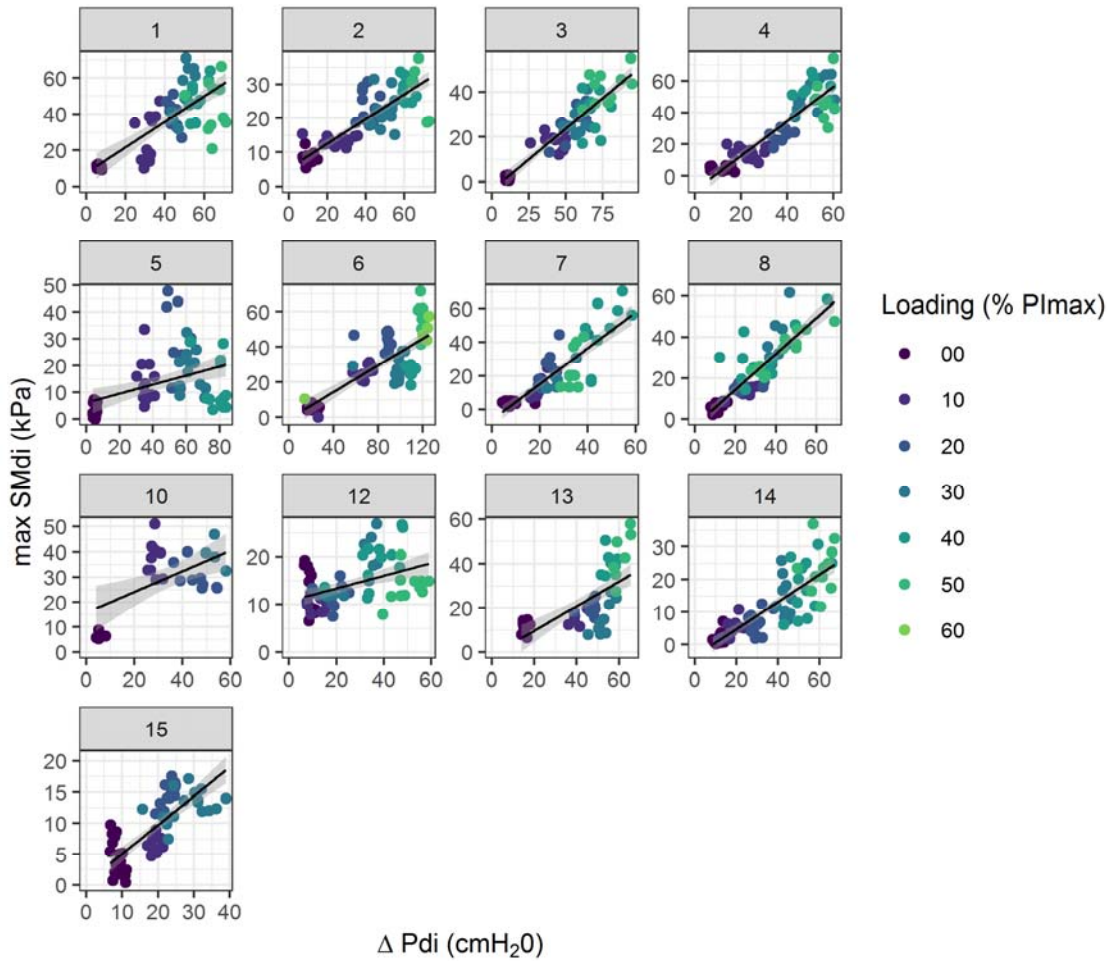
419 **Figure 6.** Relationship between transdiaphragmatic pressure and diaphragm shear modulus during unloaded
 420 ventilation and ventilation against inspiratory threshold loading (n=15).



421
 422 Panel (a): average values per condition i.e. spontaneous ventilation capacity and ventilation against inspiratory
 423 threshold loading at 10, 20, 30, 40, 50 % of maximal inspiratory pressure (PI_{max}). Panel (b): all data points
 424 with individual linear regression lines. $\max SM_{di}$, maximal diaphragm shear modulus during the inspiratory
 425 time; ΔP_{di} , variation (swing) of transdiaphragmatic pressure during the inspiratory time.

Diaphragm shear modulus reflects transdiaphragmatic pressure

426 **Figure 7.** Individual data points illustrating relationship between transdiaphragmatic pressure and diaphragm
427 shear modulus during unloaded ventilation and ventilation against inspiratory threshold loading.



428
429 max SMdi, maximal diaphragm shear modulus during the inspiratory time; Δ Pdi, variation (swing) of
430 transdiaphragmatic pressure during the inspiratory time; loading (% PImax), inspiratory threshold loading
431 expressed as a percentage of maximal inspiratory pressure.

432

